Metal Hydroxide Assisted Integrated Direct Air Capture and Conversion to Methane with Ni/Al_2O_3 catalysts

Christopher J. Koch, Vicente Galvan, Alain Goeppert, G. K. Surya Prakash*

Methods to synthesize sustainable and renewable methane are becoming of growing interest to relieve humankind from its reliance on fossil and finite natural gas reserves. Metal hydroxide salts are able to capture CO_2 from dilute sources including ambient air in the form of carbonate and bicarbonate salts. We report herein the direct conversion of such inorganic carbonate salts into methane in yields of up to 100% utilizing both Ni/Al_2O_3 and $Ni/CaAl_2O_4$ catalysts. This conversion is achieved in 48 hours with 50 bar of hydrogen at a relatively moderate temperature of 225°C under batch conditions. Water was also shown to improve the conversion of the carbonate salt to methane and the Ni/Al_2O_3 catalyst retained 99% of its activity in the alkaline media after five consecutive hydrogenation cycles. Remarkably, the metal hydroxide was also regenerated during the reaction and was reused to capture CO_2 for subsequent reactions. Compared to the conventional sequential approach involving the capture of CO_2 followed by the release of CO_2 and its hydrogenation to methane in the Sabatier reaction, the integrated route presented here can offer a number of energetic and economic benefits, paving the way for a robust carbon capture and conversion process.

https://doi.org/10.1039/D2GC04652K

A number of carbon capture technologies are being developed as strategies to limit unabated climate change from continuing.1 Carbon Capture and Sequestration (CCS) captures CO_2 from various sources including flue gases, industrial exhausts as well as the atmosphere and stores it underground in suitable geological formation or through reaction with appropriate minerals (mineralization).[2–4] Carbon Capture and Utilization (CCU), on the other hand, captures CO_2 from these same sources and proposes to use the CO_2 either as such or as a feedstock for numerous products including fuels, chemicals and plastics.[5–7] Both CCS and CCU rely on CO_2 capture processes that differ depending on parameters such as the CO_2 source, CO_2 concentration and purity. In CCU, capture and utilization/recycling have for the most part been conducted as two distinct operations that follow a sequential pathway, where CO_2 is first captured in a capture media. The captured CO_2 is then released from this capture media in an energy intensive desorption/regeneration step. Subsequently, the obtained CO_2 is compressed to be used as is, sequestered, and/or transformed into fuels and materials. The CO_2 desorption step is an endothermic process and often the energy intensive step in the overall process. It is only recently that scientists started looking into the possibility of combining capture and utilization. The integrated carbon capture and utilization (ICCU) protocols pursued by our group and others should reduce the overall energy needs of the process and lower both operational and capital expenses through process intensification. ICCU of CO_2 leads to value-added products such as methanol, formate, formamide, dimethyl ether, carbon monoxide and methane.[8–14] Methane in particular is the main component of natural gas that constitutes a large proportion of the energy consumed around the world, accounting for example for 34% of the primary energy consumption in the United States.[15] Thus, providing new pathways to synthesize methane from CO_2 and green hydrogen, where the CO_2 is captured from point sources and the atmosphere would lead to green methane, while allowing for the continued use of the vast infrastructure already in place for natural gas distribution. Carbon recycling would reduce the environmental impact of natural gas/methane and allow it to become increasingly renewable and carbon neutral.

Most of the routes currently proposed to produce methane from CO_2 rely on the sequential CCU approach described above where CO_2 is first captured and then released in an energy demanding step from the capture media at a high concentration before being hydrogenated to methane at 300-400 °C following the well-established Sabatier reaction.

In contrast to that approach, combining carbon dioxide capture with methane synthesis in an integrated process is a relatively novel concept. It has previously been reported by Heldebrant et al.[16] in a system utilizing primary and secondary amines to capture CO_2 and then convert the captured product to methane using heterogeneous ruthenium catalysts and hydrogen. Amines have been well studied as carbon capture agents, especially in homogenous systems.[17–19] However, amines have volatility and toxicity issues and often suffer from oxidative degradation.[20–23] Thus, precautions need to be taken when amines are used for the capture of CO_2, especially from air. This system also utilized ruthenium metal to catalyze the reaction. However, earth abundant metals, like nickel have also been shown to perform methanation reactions.[24–27]

Capturing CO_2 with metal hydroxides to form bicarbonate or carbonate salts has also been researched and circumvents some of the issues with amine based systems including the discussed volatility and degradation concerns.[28,29] Recently, it was reported by Prakash et al. that bicarbonate salts can be hydrogenated to methanol over a $Cu/ZnO/Al_2O_3$ catalyst.[30] Using this catalyst, the paper also showed that CO_2 can be captured from air by a metal hydroxide solution in ethylene glycol and directly converted to methanol with a yield of 97%. This example of integrated capture and conversion inspired us to explore the possibility of using a similar approach to obtain other products beside methanol; in this case methane, in high yields.

Converting inorganic carbonates and bicarbonates to methane has been previously reported in flow systems.[31–33] However, these systems often utilize temperatures above 500 °C raising their energetic costs. Some of the previous accounts using flow reactor conditions have been performed with earth abundant metals, like nickel. However, current ICCU with heterogeneous catalysts more commonly utilize rare-earth catalysts, such as ruthenium and iridium.[10,16]

The Direct Air Capture of carbon dioxide (DAC) utilizing a hydroxide salt and the subsequent conversion of the obtained metal carbonate salt to methane is a process of importance. It would circumvent the volatility problems of amine-based sorbents and could be designed in such a way to avoid base deactivation as the choice of solvent should be less constrained.[34] Current attempts in utilizing this technology typically use bifunctional solid materials composed of an alkali metal containing species and a catalyst. The alkali metal species on the surface reacts with CO_2 to form a carbonate/bicarbonate salt. This salt is then decomposed to form CO_2 again before the reaction occurs.[24,35–37] As the catalysts used are generally air sensitive, this means that the catalyst in these bifunctional materials need to be regenerated under hydrogen during each adsorption/conversion cycle. This consumes part of the hydrogen and is rather energy intensive. At the same time, a large amount of catalyst is also tied up in the adsorbent material during the adsorption period, which could be capital intensive, especially if the catalyst is based on precious metals. Thus, it could be advantageous to decouple the capture and conversion steps. In the first step, CO_2 is captured with a strong base in the form of a carbonate/bicarbonate salt. In a second, separate but adjacent, step this salt is converted to methane over a catalyst. In doing so, the catalyst is always in the hydrogenation mode and does not

require regeneration in each recurring adsorption/conversion cycle. It should allow for a more efficient use of the catalyst and reduce the amount of catalyst needed and therefore cost of the overall process.

Herein, we report the direct hydrogenative conversion of potassium bicarbonate and carbonate to methane at relatively low temperatures and the concurrent regeneration of the hydroxide base utilizing both Ni/Al_2O_3 and $Ni/CaAl_2O_4$ catalysts. This reaction can also be undertaken with carbonate and bicarbonate salts synthesized directly from the atmospheric air using an alkali metal hydroxide thus decoupling capture and conversion. The catalyst can then be easily separated from the base after the reaction and both components be used again in subsequent reaction cycles (Figure 1). Interestingly, the reaction does not consume more hydrogen as compared to the simple hydrogenation of CO_2 to methane with the added benefit of regenerating the base that can be reused for subsequent CO_2 capture (Figure 2, Sabatier reaction).

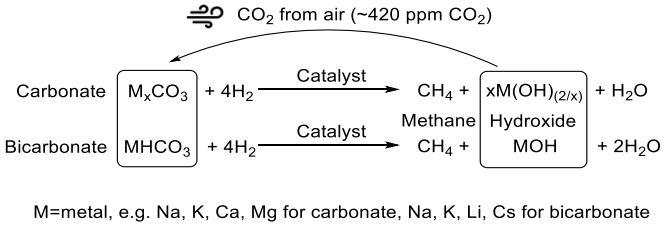

Figure 1. Direct air capture of CO_2 with a metal hydroxide and hydrogenation of the obtained carbonate/bicarbonate to methane with concurrent recycling of the base.

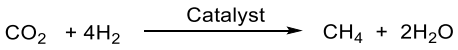

Figure 2. Hydrogenation of CO_2 to methane (Sabatier reaction).

Results and Discussions

To test the activity of the catalyst for hydrogenation, potassium bicarbonate was used as a model substrate. Ethylene glycol had previously been reported as an optimal solvent for the integrated capture and conversion of CO_2 to methanol. However, ethylene glycol has also been reported to reform and decompose to $CH_4/CO/CO_2$ under the reaction conditions used in our work.[38–40] Indeed, when a blank hydrogenation reaction was performed with only ethylene glycol and the nickel-based catalyst, we observed the formation of $CH_4/CO/CO_2$. Thus, water was used as a solvent to avoid these issues and any additional carbon source in the system. In a first series of experiments, a commercial steam reforming catalyst, $Ni/CaAl_2O_4$ (HiFUEL R110, Alfa Aesar), was utilized for the hydrogenation of bicarbonate salts.[41] Optimization results are presented in Table 1. Temperature was an important parameter for the reaction, as both 170 and 200°C showed very little conversion to methane at 6 and 7%, respectively. Only upon reaching 225°C, did the reaction proceed to methane with a much higher yield of up to 97% with $KHCO_3$. This resulted in the highest methane productivity of 10.8 $g_{methane} \cdot h^{-1} \cdot kg_{cat}^{-1}$, which was calculated using similar methods reported previously.[13,24] Under these conditions, both decreasing or increasing the H_2 pressure below or above 50 bar had a negative effect on the methane yield. Lowering the reaction time from 48 to 24h greatly diminished the methane yield. K_2CO_3 was also hydrogenated to methane, although with a yield that was about half the one observed with KHCO3 after 48h under similar reaction conditions. Interestingly, even in the absence of water, $KHCO_3$ was converted to methane with a yield of 48% compared to no conversion for K_2CO_3.

Table 1. Hydrogenation of $KHCO_3$ and K_2CO_3 to methane over $Ni/CaAl_2O_4$

Entry	Salt	Amount of salt (mmol)	H_2 pressure (bar)	Temperature (°C)	Time (hours)	Methane yield (mmol)	Methane yield (%)	Methane productivity $g_{methane} \cdot h^{-1} \cdot kg_{cat}^{-1}$
1	$KHCO_3$	10	50	170	48	0.6	6	0.67
2	$KHCO_3$	10	50	200	48	0.7	7	0.78
3	$KHCO_3$	10	50	225	48	9.7	97	10.8
4	$KHCO_3$	10	40	225	48	5.4	54	6.0
6	$KHCO_3$	10	60	225	48	8.2	82	9.1
7	$KHCO_3$	10	70	225	48	6.3	63	7.0
8	$KHCO_3$	10	50	225	24	2.2	22	4.9
9	$KHCO_3$	10	50	225	72	9.8	98	7.3
10	K_2CO_3	10	50	225	48	5.3	53	5.9
11	$KHCO_3$[a]	10	50	225	48	4.8	48	5.4
12	K_2CO_3[a]	10	50	225	50	0	0	0

Reaction conditions: water (10 mL), H_2 pressure at room temperature, 300 mg $Ni/CaAl_2O_4$. [a] water (0 mL). Methane yields calculated relative to the carbonate as determined by Gas chromatography. Yield calculations ± 5%.

The $Ni/CaAl_2O_4$ catalyst was subsequently tested over several cycles to assess its reusability and stability. Captured CO_2 was used in the recycling experiments. 4 mmol of KOH was dissolved in water and pure CO_2 was contacted with the salt solution for three hours. The amount of captured CO_2 in the form of a carbonate/bicarbonate mixture was quantified by ^{13}C NMR. After capture, the obtained potassium carbonate/bicarbonate was subjected to hydrogenation using the conditions in entry 3 of Table 1. In the first cycle, 3.23 mmol of methane was obtained from 4 mmol of CO_2 captured. The liquid aqueous solution after reaction was separated from the solid catalyst and subjected to CO_2 capture, capturing 2.75 mmol of CO_2 and demonstrating the regeneration of the KOH base in the hydrogenation process. The obtained aqueous solution was then subjected to hydrogenation in a second cycle using the same catalyst as in the first cycle. After that, the capture/hydrogenation was repeated 3 more times. The results of the recycling studies are shown in Table 2. After five cycles, the amount of base had decreased from the original 4 mmol to 2 mmol. Consequently, while the conversion of CO_2 to methane remained relatively constant in the ~90-100% range after the initial cycle, the lower carbonate content led to a decrease in the amount of methane that can be formed in each cycle. Thus, at some point in the reaction, the base is deactivated or converted to a product that is less able to capture CO_2.

Table 2. Recycling experiments of the $Ni/CaAl_2O_4$ catalyst and KOH base for methane production over 5 absorption/hydrogenation cycles

Cycle	Amount of CO_2 captured (mmol)	Conversion to methane (mmol)	Conversion to methane (%)	Capture regeneration (%)[a]
1	4.03	3.23	80.1	-
2	2.75	2.70	98.2	68.2
3	2.4	2.25	93.8	87.3
4	2.24	2.07	92.0	93.8
5	2.05	1.98	96.6	91.1

Reaction conditions: water (10 mL), 50 bar H_2 pressure at room temperature, 300 mg $Ni/CaAl_2O_4$, 48 hours, initial amount of KOH: 4 mmol. Methane yields calculated relative to the carbonate as determined by Gas chromatography. Yield calculations ± 5%. [a] compared to CO_2 absorption in previous cycle.

It has been previously reported that calcium present in $Ni/CaAl_2O_4$ can interact with metal carbonates to form calcium carbonate, which is less soluble and could be a contributing factor to the loss of capture regeneration over the course of the five reactions.[36,37] The relevant reactions are shown in Figure 3. Having a decreased amount of potassium hydroxide with an increased amount of calcium hydroxide in the solution negatively effects the CO_2 capture step after the reaction. It has been reported that potassium hydroxide is able to capture CO_2 much faster than calcium hydroxide.[18] This is consistent with our results where potassium peaks are present in the XRD of the catalyst after the reaction as shown in Figure S1.

$$CaAl_2O_4 + K_2CO_3 \longrightarrow 2KAlO_2 + CaCO_3$$
$$CaAl_4O_7 + K_2CO_3 + 2KOH + 7H_2O \longrightarrow 4KAl(OH)_4 + CaCO_3$$
$$Ca_3Al_2O_6 + 3K_2CO_3 + 2H_2O \longrightarrow 2KAlO_2 + 3CaCO_3 + 4KOH$$
$$Ca_{12}Al_{14}O_{33} + 12K_2CO_3 + 5H_2O \longrightarrow 14KAlO_2 + 12CaCO_3 + 10KOH$$

Figure 3. Depiction of a possible deactivation pathways on the catalyst surface for $Ni/CaAl_2O_4$.[42-43]

To limit the base deactivation due to the composition of the $Ni/CaAl_2O_4$ catalyst, a Ni/Al_2O_3 catalyst was synthesized containing 25% nickel by weight as confirmed by X-Ray Fluorescence (XRF) (please see SI). Table 3 shows the results for the hydrogenation of metal carbonates and bicarbonates utilizing this catalyst. The yield for $KHCO_3$ was similar to the one obtained with $Ni/CaAl_2O_4$ (100% vs 97% on $Ni/CaAl_2O_4$). However, the yield of methane when utilizing potassium carbonate was greatly improved from 53% with $Ni/CaAl_2O_4$ to 100% with 25%Ni/Al_2O_3. This also led to a corresponding increase in methane productivity from 5.9 to 11.1 $g_{methane}\cdot h^{-1}\cdot kg_{cat}^{-1}$ from the $Ni/CaAl_2O_4$ to $Ni/Al2O_3$. This difference is most likely due to the K_2CO_3 interacting with the calcium in the former $Ni/CaAl_2O_4$ catalyst and thus deactivating the catalyst. Due to the absence of calcium in Ni/Al2O3 this reaction is not possible. The productivity with Ni/Al_2O_3 was further improved to 12.3 $g_{methane}\cdot h^{-1}\cdot kg_{cat}^{-1}$ when 20 mmol of potassium carbonate was used instead of 10 mmol, although at a lower overall methane yield of only 55%. Other carbonate salts, like sodium carbonate and cesium carbonate can also be utilized resulting in quantitative yields as well. Calcium carbonate performed significantly worse than the aforementioned carbonate salts with a 5% yield of methane. In an attempt to increase the yield with calcium carbonate, a small portion of potassium carbonate was added. This was done in the hope that the resulting potassium hydroxide would leach the calcium carbonate and create potassium carbonate. However, this seemingly did not occur as the methane yield remained relatively low at 15%. When a ^{13}C-labelled potassium carbonate salt was used in the reaction, the result was the formation of ^{13}C-methane as determined by NMR and shown in Figure S12 and S13.

Table 3. Hydrogenation of metal bicarbonate and carbonate to methane over Ni/Al_2O_3 (25 wt% Ni)

Salt	Amount (mmol)	Hydrogen pressure (bar)	Temperature (°C)	Time (hours)	Water (mL)	Methane yield (mmol)	Methane yield (%)	Methane productivit $g_{methane}\cdot h^{-1}\cdot kg_{cat}^{-1}$
$KHCO_3$	10	50	225	48	10	10	100	11.1
K_2CO_3	10	50	225	48	10	10	100	11.1
$K_2{}^{13}CO_3$	10	50	225	48	10	10	100	11.1
K_2CO_3	20	50	225	48	10	11	55	12.3
Na_2CO_3	10	50	225	48	10	10	100	11.1
Li_2CO_3	10	50	225	48	10	9.1	91	10.1
Cs_2CO_3	10	50	225	48	10	10	100	11.1

$CaCO_3$	10	50	225	48	10	0.5	5	0.6
$CaCO_3/K_2CO_3$[a]	10	50	225	48	10	1.5	15	1.7

Reaction conditions: water (10 mL), 50 bar H_2 pressure at room temperature, 300 mg Ni/Al_2O_3 [a] 9.0 mmol $CaCO_3$ and 1.0 mmol K_2CO_3. Methane yields calculated relative to the carbonate as determined by Gas chromatography. Yield calculations ± 5%.

The stability of the Ni/Al_2O_3 catalyst was then tested over five absorption/hydrogenation cycles using a similar procedure as employed with $Ni/CaAl_2O_4$ but starting with 4 mmol of KOH. In this case, the reactivity remained consistent and 99% of the catalyst activity was retained at the end of five cycles. Again, CO_2 captured by the KOH regenerated during the hydrogenation step was utilized in the form of carbonate in the subsequent cycle. There was no decrease in catalytic activity and only a slight loss in base activity after five cycles as shown in Figure 4b. This was a clear improvement over the system based on $Ni/CaAl_2O_4$. As shown in the XRD (Figure S2), there is less of an accumulation of potassium on the catalyst surface after the reaction. This means that the catalyst surface is less affected over the course of the reaction. The support in the $Ni/CaAl_2O_4$ also deteriorates over the course of the reaction, whereas the alumina in Ni/Al_2O_3 is relatively unaffected by the reaction as shown in Figure S2. The $Ni/CaAl_2O_4$ has potassium peaks in the XRD after the reaction. This also corresponds to the grossite ($CaAl_4O_7$) peaks in the XRD disappearing as compared to the XRD of the catalyst before reaction.

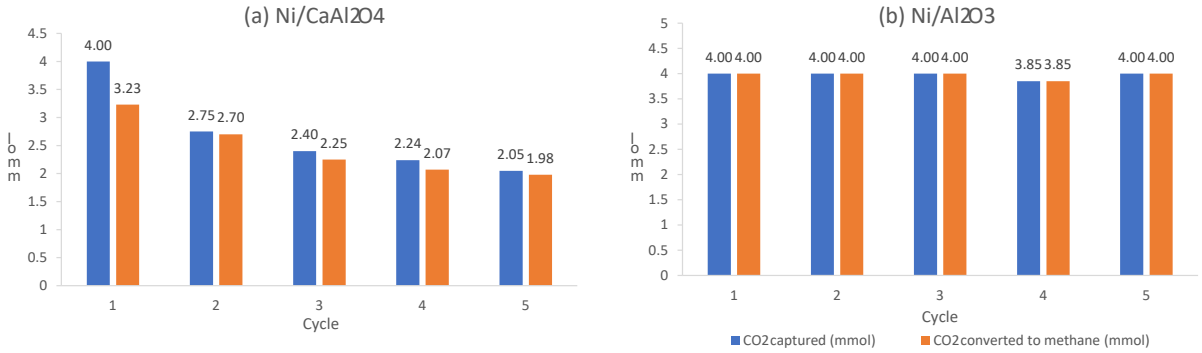

Figure 4. Recycling studies of potassium hydroxide/carbonate for methane production using (a) $Ni/CaAl_2O_4$ and (b) Ni/Al_2O_3.

Figures 4a and 4b compare the recyclability of the $Ni/CaAl_2O_4$ and Ni/Al_2O_3 catalysts and how these catalysts performed over five absorption/hydrogenation cycles. The graphs show that the system with $Ni/CaAl_2O_4$ exhibits both catalytic deactivation and base loss. In contrast, the system with Ni/Al_2O_3 only exhibits a marginal loss of base. In the case of Ni/Al_2O_3 the recycling studies showed that both the catalyst and the base can perform well over these capture/hydrogenation cycles.

Table 4. Recycling studies of the Ni/Al_2O_3 catalyst and the KOH base for methane production over 5 absorption/hydrogenation cycles

Cycle	Amount CO_2 captured (mmol)	Conversion to methane (mmol)	Conversion to methane (%)	Capture regeneration (%)[a]
1	4.0	4.0	100	-
2	4.0	4.0	100	100
3	4.0	4.0	100	100
4	3.85	3.85	100	96.3

5	4.0	4.0	100	103.9

Reaction conditions: capture solution (10 mL), 50 bar H_2 pressure at room temperature, 300 mg Ni/Al_2O_3, 4 mmol KOH. Methane yields calculated relative to the carbonate as determined by Gas chromatography. Yield calculations ± 5%. [a] compared to CO_2 absorption in previous cycle.

Table 5 shows that the direct capture of CO_2 from the air and its conversion to methane is also possible in high yields. 5 mmol of KOH was used in 10 mL of water to capture 3.53 mmol of CO_2 from air in the form of a bicarbonate/carbonate mixture. This salt was then converted quantitatively to methane over Ni/Al_2O_3 in 48h. To confirm that the base was regenerated, a titration with CO_2 as the acid was performed with the aqueous solution after reaction. The titration resulted in 3.5 mmol of CO_2 being captured demonstrating that the base had therefore been fully regenerated during the hydrogenation reaction.

Table 5. Direct air capture and conversion to methane utilizing a KOH base and Ni/Al_2O_3 catalyst

Amount of KOH (mmol)	Amount CO_2 captured (mmol)	Conversion to methane (mmol)	Conversion to methane (%)
5	3.53	3.53	100

Reaction conditions: capture solution (10 mL), 48 hours, 50 bar H_2 pressure at room temperature, 300 mg Ni/Al_2O_3. Methane yields calculated relative to the carbonate as determined by Gas chromatography. Yield calculations ± 5%.

While the ICCU route described in this report holds promise, it should be noted that it is still at an early stage (technology readiness level (TRL) of about 3) and will require much more development before becoming practical on a larger scale. A continuous process would for example be preferable to the batch approach used here. Shortening of the reaction time by employing improved or different and more active catalysts should also be pursued to improve throughput, productivity, and reduce the energy required to maintain the reactor temperature. To reduce the energy needed for hydrogen compression reaction at a lower pressure, if possible, would be advantageous as well.

The process is also only as green as the feedstock and energy used to run it. As the process matures, care should thus be taken in using renewable sources of energy for all parts of the process including CO_2 capture, hydrogen generation, the hydrogenation reaction, product separation, etc. As for any other proposed low carbon process, a life cycle analysis should also validate the “greenness” of the approach in terms of greenhouse gas emissions, carbon footprint and overall environmental impacts. To be sustainable in the long run CO_2 captured from the atmosphere would be an ideal source for this route. A lot of the DAC technologies such as the one based on metal hydroxides as the capturing media rely on fans to push air through the capturing media.44-45 Minimizing pressure drop through this aqueous media during CO_2 adsorption through proper equipment design and engineering is thus also a crucial aspect to reduce the energy needs of the fans and the entire ICCU process. Although less efficient for DAC, pools of hydroxides could potentially also be employed to eliminate the need for fans. Spays of capturing media have been proposed as well to reduce the pressure drop.

Conclusions

We have shown here that the conversion of carbonate salts of potassium and sodium directly to methane can be achieved in high yield and selectivity over heterogeneous catalysts. Because this process is performed in an aqueous solution, it does not suffer from base deactivation that was for instance observed in the homologous methanol synthesis from carbonates, which is carried out in ethylene glycol. High degree of recycling of both the catalyst and base was demonstrated. Thus, this reaction has the potential deliver large number of CO_2 absorption/hydrogenation cycles. Direct air capture of CO2 and conversion to methane was also achieved with KOH as the base, demonstrating that the synthesis of methane can be effectively performed with atmospheric CO_2. This opens a pathway to potentially synthesize renewable methane with a lower or even neutral carbon footprint through an anthropogenic carbon cycle analogous to nature's own photosynthetic cycle. This is also a three-phase reaction system (solid, liquid, gas) that can offer some advantages. The capture media can be easily separated from the catalyst and allows for easy access for the media to capture CO_2 again while leaving the catalyst unaffected. The product, methane, is also easy to separate due to its gaseous nature.

Acknowledgment

Support of our work by the Loker Hydrocarbon Research Institute at the University of Southern California is gratefully acknowledged. We would like to thank the National Science Foundation (award: CHE-2018740) for the purchase of the diffractometer used to obtain powder diffraction patterns reported here. We would also like to thank the Center of Excellence for Nano Imaging (CNI) at the University of Southern California for microscope time and access to the XRF.

Author Contributions

Corresponding Author:* gprakash@usc.edu

ORCID:

Christopher J Koch: 0000-0003-0565-6853

Vicente Galvan: 0000-0001-9009-8846

Alain Goeppert: 0000-0001-8667-8530

G. K. Surya Prakash: 0000-0002-6350-8325

Conflicts of interest

The authors declare no competing financial interest.

Notes and references

1 J. Rissman, C. Bataille, E. Masanet, N. Aden, W. R. Morrow, N. Zhou, N. Elliott, R. Dell, N. Heeren, B. Huckestein, J. Cresko, S. A. Miller, J. Roy, P. Fennell, B. Cremmins, T. Koch Blank, D. Hone, E. D. Williams, S. de la Rue du Can, B. Sisson, M. Williams, J. Katzenberger, D. Burtraw, G. Sethi, H. Ping, D. Danielson, H. Lu, T. Lorber, J. Dinkel and J. Helseth, Appl Energy, 2020, 266, 114848.

2 S. Chu, Science (1979), 2009, 325, 1599.

3 E. J. Wilson, S. J. Friedmann and M. F. Pollak, Environ Sci Technol, 2007, 41, 5945–5952.

4 H. Pilorgé, N. McQueen, D. Maynard, P. Psarras, J. He, T. Rufael and J. Wilcox, Environ Sci Technol, 2020, 54, 7524–7532.

5 M. Mahmoudkhani and D. W. Keith, International J Greenh Gas Control, 2009, 3, 376–384.

6 J. K. Stolaroff, D. W. Keith and G. v Lowry, Environ Sci Technol, 2008, 42, 2728–2735.

7 L. Lu, J. S. Guest, C. A. Peters, X. Zhu, G. H. Rau and Z. J. Ren, Nat Sustain, 2018, 1, 750–758.

8 J. Kothandaraman and D. J. Heldebrant, Green Chem., 2020, 22, 828–834.

9 S. Kar, A. Goeppert and G. K. S. Prakash, Acc Chem Res, 2019, 52, 2892–2903.

10 D. Cheng, M. Wang, L. Tang, Z. Gao, X. Qin, Y. Gao, D. Xiao, W. Zhou and D. Ma, Angew Chem Int Ed, 2022, 61, e202202654.

11 G. Wang, Y. Guo, J. Yu, F. Liu, J. Sun, X. Wang, T. Wang and C. Zhao, Chem Eng J, 2022, 428, 132110.

12 R. Sen, A. Goeppert and G. K. S. Prakash, J Organomet Chem, 2022, 965–966, 122331.

13 R. Sen, C. J. Koch, V. Galvan, N. Entesari, A. Goeppert and G. K. S. Prakash, J CO2 Util, 54, 101762.

14 S. Kar, A. Goeppert and G. K. S. Prakash, ChemSusChem, 2019, 12, 3172–3177.

15 U. Energy Information Administration, Monthly Energy Review - September 28, 2022.

16 J. Kothandaraman, J. Saavedra Lopez, Y. Jiang, E. D. Walter, S. D. Burton, R. A. Dagle and D. J. Heldebrant, ChemSusChem, 2021, 14, 4812–4819.

17 R. Sen, C. J. Koch, A. Goeppert and G. K. S. Prakash, ChemSusChem, 2020, 13, 6318–6322.

18 J. Kothandaraman, S. Kar, R. Sen, A. Goeppert, G. A. Olah and G. K. S. Prakash, J Am Chem Soc, 2017, 139, 2549–2552.

19 S. Kar, R. Sen, J. Kothandaraman, A. Goeppert, R. Chowdhury, S. B. Munoz, R. Haiges and G. K. S. Prakash, J Am Chem Soc, 2019, 141, 3160–3170.

20 A. Goeppert, H. Zhang, R. Sen, H. Dang and G. K. S. Prakash, ChemSusChem, 2019, 12, 1712–1723.

21 S. B. Fredriksen and K.-J. Jens, Energy Proc, 2013, 37, 1770–1777.

22 F. Vega, A. Sanna, B. Navarrete, M. M. Maroto-Valer and V. J. Cortés, Greenh Gases Sci Technol, 4, 707–733.

23 M. Jahandar Lashaki, S. Khiavi and A. Sayari, Chem. Soc. Rev., 2019, 48, 3320–3405.

24 J. A. Onrubia-Calvo, A. Bermejo-López, S. Pérez-Vázquez, B. Pereda-Ayo, J. A. González-Marcos and J. R. González-Velasco, Fuel, 2022, 320, 123842.25

25 H.-W. Chen, C.-Y. Wang, C.-H. Yu, L.-T. Tseng and P.-H. Liao, Catal Today, 2004, 97, 173–180.

26 M. S. Lanre, A. S. Al-Fatesh, A. H. Fakeeha, S. O. Kasim, A. A. Ibrahim, A. S. Al-Awadi, A. A. Al-Zahrani and A. E. Abasaeed, Processes, 2020, 8, 1–15.

27 C. J. Koch, A. Alagaratnam, A. Goeppert and G. K. S. Prakash, Isr J Chem, 2023, DOI:10.1002/ijch.202200119.

28 Y. Du, Y. Yuan and G. T. Rochelle, Int. J. Greenh Gas Control, 2017, 58, 1–9.

29 R. Sen, A. Goeppert, S. Kar and G. K. S. Prakash, J Am Chem Soc, 2020, 142, 4544–4549.

30 R. Sen, C. J. Koch, V. Galvan, N. Entesari, A. Goeppert and G. K. S. Prakash, J of CO2 Util, 2021, 54, 101762.

31 D. Jagadeesan, M. Eswaramoorthy and C. N. R. Rao, ChemSusChem, 2009, 2, 878–882.

32 S. Lux, G. Baldauf-Sommerbauer and M. Siebenhofer, ChemSusChem, 2018, 11, 3357–3375.

33 S. Zhang, H.-Q. Chen, X. Kan, Y.-L. Tai, W.-L. Liu, B.-X. Dong and Y.-L. Teng, Fuel, 2021, 292, 120395.

34 Y. Song, X. Cui, T. Deng, Z. Qin, W. Fan, J Fuel Chem Technol, 2021, 49, 178–185.

35 C. Jeong-Potter, M. Abdallah, C. Sanderson, M. Goldman, R. Gupta and R. Farrauto, Appl Catal B, 2022, 307, 120990.

36 S. Jo, J. H. Lee, T. Y. Kim, J. H. Woo, H.-J. Ryu, B. Hwang, S. C. Lee, J. C. Kim and K. L. Gilliard-AbdulAziz, Fuel, 2022, 311, 122602.

37 S. J. Park, M. P. Bukhovko and C. W. Jones, Chem Eng J, 2021, 420, 130369.

38 R. R. Davda, J. W. Shabaker, G. W. Huber, R. D. Cortright and J. A. Dumesic, Appl Catal B, 2003, 43, 13–26.

39 J. W. Shabaker, G. W. Huber, R. R. Davda, R. D. Cortright and J. A. Dumesic, Catal Letters, 2003, 88, 1–8.

40 S. Kandoi, J. Greeley, D. Simonetti, J. Shabaker, J. A. Dumesic and M. Mavrikakis, J Phys Chem C, 2011, 115, 961–971.

41 H. P. Hamers, F. Gallucci, G. Williams, P. D. Cobden and M. van Sint Annaland, Energy Fuels, 2015, 29, 2656–2663.

42 F. I. Azof, M. Vafeias, D. Panias and J. Safarian, Hydrometallurgy, 2020, 191, 105184.

43 F. I. Azof, Y. Yang, D. Panias, L. Kolbeinsen and J. Safarian, Hydrometallurgy, 2019, 185, 273–290.

44 A. Goeppert, M. Czaun, G. K. S. Prakash and G. A. Olah, Energy Environ. Sci., 2012, 5, 7833–7853.

45 E. S. Sanz-Pérez, C. R. Murdock, S. A. Didas and C. W. Jones, Chem Rev., 2016, 116, 11840–11876.

Metal Hydroxide Assisted Integrated Direct Air Capture and Conversion to Methane with Ni/Al_2O_3 catalysts

Christopher J. Koch, Vicente Galvan, Alain Goeppert, G.K. Surya Prakash*

1. Experimental part

1.1 Materials and Methods

All experiments were carried out under an inert atmosphere (with N_2 or Ar) using standard Schlenk techniques with the exclusion of moisture unless otherwise stated. Commercial $Ni/CaAl_2O_4$ catalyst was purchased from Alfa Aesar (HiFUEL R110). Nickel nitrate hexahydrate ($Ni(NO_3)_2 \cdot 6H_2O$) (99.9% purity) was purchased from Alfa Aesar. Fumed alumina , Al_2O_3, Aeroxide AluC, was obtained from Evonik. Potassium carbonate, potassium bicarbonate, sodium carbonate, lithium carbonate, cesium carbonate and calcium carbonate were purchased from Sigma Aldrich, had all a purity of 99.9% or higher, and were used without further purification. Potassium hydroxide was purchased from Sigma Aldrich and had a purity of 97%. ^{13}C-labelled potassium carbonate was purchased from Stable Isotopes with a purity of 98.7%, D_2O (CIL, D-99.9%), toluene-d_8 (CIL, 99.5%) and imidazole (Fischer, 99.5%) were used as received. ^1H and ^{13}C NMR spectra were recorded on 400, 500 or 600 MHz, Varian NMR spectrometers. ^1H and ^{13}C NMR chemical shifts were determined relative to the residual solvent signals. The gas mixtures were analyzed using a Thermo Finnigan gas chromatograph (column: Supelco, Carboxen 1010 plot, 30 m X 0.53 mm) equipped with a TCD detector (CO detection limit: 0.099 v/v%). CO_2 (Gilmore, instrument grade), H_2 (Gilmore, ultra-high pure grade 5.0), Methane (Gilmore, instrument grade), and ^{13}C-Methane (Monsanto Research Corporation, 99%) were used without further purification.

Caution: Reactions are associated with H_2 gas. They should be carefully handled inside proper fume hoods without any flame, spark or static electricity sources nearby.

1.2 Catalyst synthesis

3.3 g of nickel nitrate hexahydrate ($Ni(NO_3)_2 \cdot 6H_2O$) was dissolved into 100 mL of DI water. 6.7g of fumed Al_2O_3 was then added to the solution, forming a suspension. The solution was stirred for 5 hours. Water was then removed with a rotavapor and the obtained solid dried overnight in an oven at 120°C. The dried material was then calcinated at 700°C for 2 hours after heating it from room temperature to 700°C at a rate of 5.8°C/min under an atmosphere of air.

1.3 Catalyst activation

The catalyst (prepared and calcinated Ni/Al_2O_3 or commercial $Ni/CaAl_2O_4$) was crushed and sieved to a size of 250 micrometers or less. The sieved material was then activated in a tubular quartz reactor placed in a tubular furnace (Lindberg Blue). Nitrogen was flown through the catalyst at a rate of 75mL/min for 30 minutes at room temperature. After that a mixture of hydrogen/nitrogen (35mL/min and 75 mL/min, respectively) was flown through the catalyst while it was heated to 700°C (5.8°C/min) and held at that temperature for 2 hours. The catalyst was then allowed to cool down and was stored in an inert atmosphere for later use.

1.4 Hydrogenation of carbonates to methane

All carbonate and bicarbonate salts were purchased with a purity of 99.9% or higher from Sigma Aldrich. The activated catalyst was weighed in an atmosphere of argon and then transported to a nitrogen chamber. There, 10 mmol of carbonate was mixed with DI water as the solvent. The catalyst, solvent (water), and carbonate salt were placed in a borosilicate vial. This vial was then placed in a 125 mL Hastelloy Parr reactor that was sealed in the nitrogen chamber. The Parr reactor was pressurized with hydrogen (UHP). Then, the reactor was placed in a pre-heated aluminum block, heated to the desired temperature and held at that temperature for the duration of the reaction. At the end of the reaction, the reactor was cooled to room temperature, the pressure was released, and the solvent was separated from the catalyst via decanting. A portion of the gas mixture was released into a gas collection bag for gas chromatography (GC) analysis. The yield was then computed by integration of the gas peaks from the GC analysis. A sample calculation is provided in section 2.2.

1.5 Air capture of CO_2 with potassium hydroxide

To capture CO_2 from air (~420 ppm CO_2) potassium hydroxide (Sigma Aldrich, 97%) was dissolved in 10 mL of DI H_2O in a vial. The vial was sealed and air from the lab was then flown through the vial at the rate of 300 mL/min. The air capture was run for 48 hours. Afterwards, tert-butanol (tBuOH) was added as an internal standard to a 0.1mL aliquot of the capture solution. This aliquot was analyzed by ^{13}C NMR with D_2O as the deuterated solvent. The amount of CO_2 was quantified through ^{13}C NMR analysis. The remaining solution was used for hydrogenation.

1.6 CO_2 from pure CO_2 capture

A known amount of alkali hydroxide (KOH) was dissolved in DI water (10 mL) in a vial with a magnetic stir bar. The gases inside the vial were then removed under vacuum. CO_2 was subsequently added while stirring the solution at 800 rpm for 3 h and maintaining the CO_2 pressure inside the reactor at 1 psi above atmospheric pressure. The amount of CO_2 captured was calculated both through the volume of CO_2 added and through gravimetric analysis of the solutions before and after the capture.

1.7 Recycling Experiments

Once the hydrogenation reaction according to the method described in 1.4 was complete the reactor was cooled down to room temperature and the pressure released. Part of the pressure was released into a collection bag for gas chromatography analysis. The reactor was then transferred to a nitrogen chamber and opened. The liquid in the reactor was separated from the catalyst by decantation and placed in a 100 mL round bottom flask. After evacuation, the subsequent capture conditions follow the same parameters as detailed in 1.6. The amount of CO_2 captured was measured by both the volume of CO_2 added and gravimetrically. The liquid was then placed back in the reactor with the catalyst that was utilized in the previous cycle. The hydrogenation reaction was then were performed again with the conditions detailed in 1.4.

1.8 Powder X-Ray Diffraction (XRD)

Powder XRD was performed on a sixth generation Rigaku Miniflex powder diffractometer. The catalyst was wet loaded onto a sample plate and then dried of any solvent. The scan was set from 10°-80° at a scan rate of 3°/min. The resulting spectrum were processed on the PDXL software.

1.9 Scanning Electron Microscopy (SEM)

Scanning Electron Microscopy (SEM) images and energy dispersive X-ray spectroscopy (EDS) images were obtained from a JEOL JSM-7001F electron microscope with an acceleration voltage of 18 keV.

1.10 X-Ray Fluorescence (XRF)

X-Ray Fluorescence (XRF) was conducted on a Bruker Tiger S8 instrument. The X-Ray source is rhodium leading to residual rhodium signals, which are labelled in the spectrum. The spectra were all collected between 0-60 keV. The weight percentages of the metals were calculated using the Bruker software and all errors of the measurements are reported. The calculations were based on the Kα peak.

2 Data

2.1 XRD data

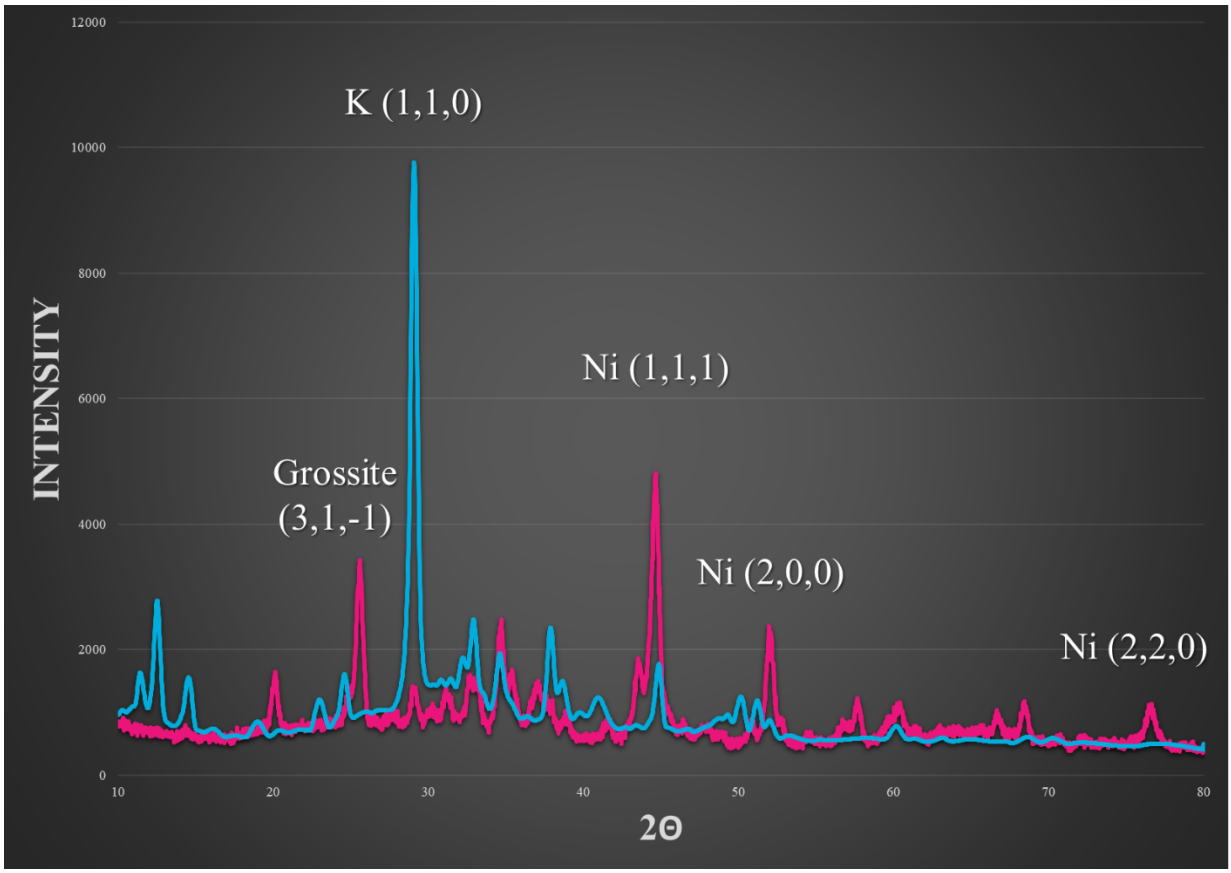

Figure S1. Powder XRD of Ni/$CaAl_2O_4$ before the reaction (shown in red) and after the reaction with potassium bicarbonate (shown in blue).

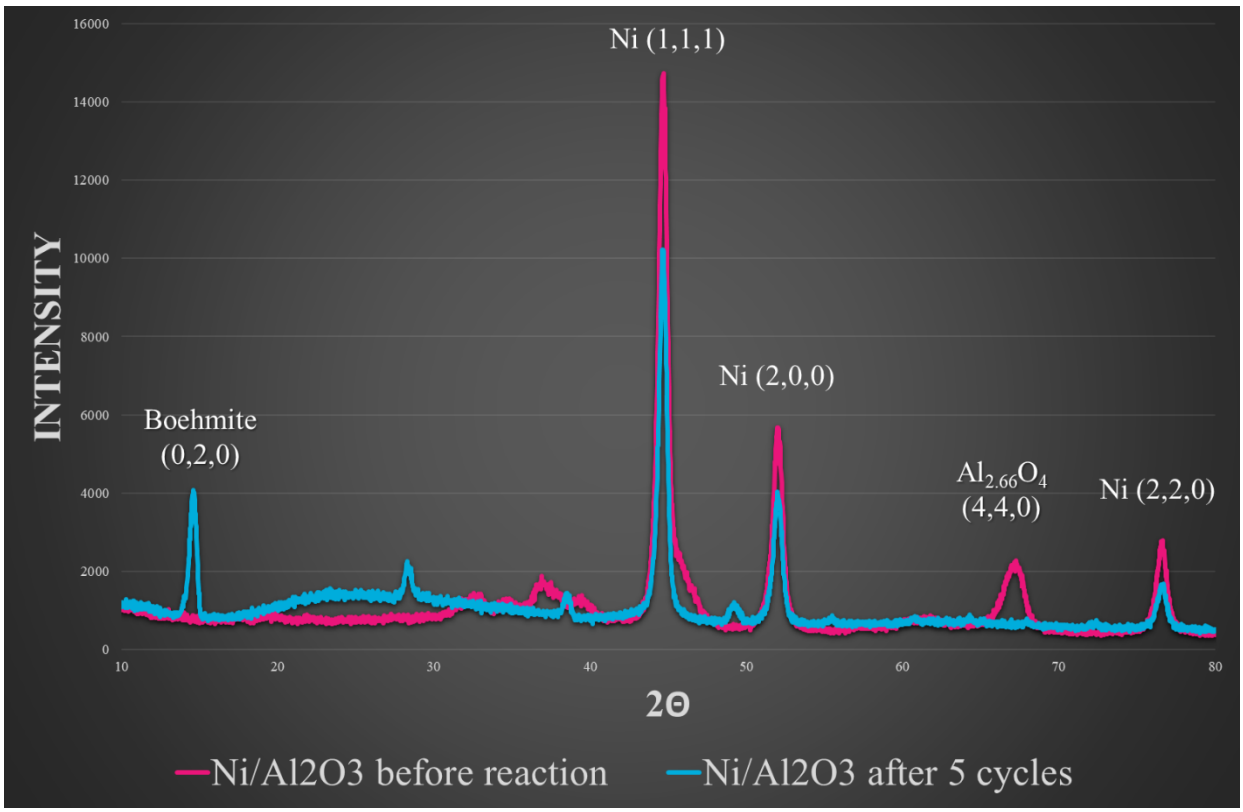

Figure S2. Powder XRD of Ni/Al_2O_3 before the reaction (shown in red) and after five cycles of the reaction (shown in blue).

Table S1. D-spacing and crystallite size of the catalyst before and after reaction

Sample	D-spacing (Å)[a]	Crystallite Size (Å)[b]
$Ni/CaAl_2O_4$ (HiFuel 110)	2.03	156
$Ni/CaAl_2O_4$ after reaction with $KHCO_3$	2.02	189
$Ni/CaAl_2O_4$ after reaction with K_2CO_3	2.03	87
$Ni/CaAl_2O_4$ after 5cycles	2.03	123
Ni/Al_2O_3	2.03	139
Ni/Al_2O_3 after reaction with $KHCO_3$	2.08	138
Ni/Al_2O_3 after reaction with K_2CO_3	2.03	166
Ni/Al_2O_3 after reaction with Na_2CO_3	2.03	147
Ni/Al_2O_3 after 5 cycles	2.03	154

[a] D-spacing was calculated by Bragg's law and all measurements are within 0.1 Å [b] crystallite size measurements are all within 1 Å.

2.2 Gas Chromatography data

Figures S3 and S4 show the standard gas chromatography, which was used for the analysis of the products. The gas chromatography shows a peak at 1.8 minutes which corresponds to hydrogen. The peak 2.2 minutes relates to nitrogen/air and the peak at 4.5 minutes corresponds to methane, the reaction product. If carbon monoxide or carbon dioxide were present a peak would appear in the gas chromatography at 2.8 minutes and 8.5 minutes, respectively.

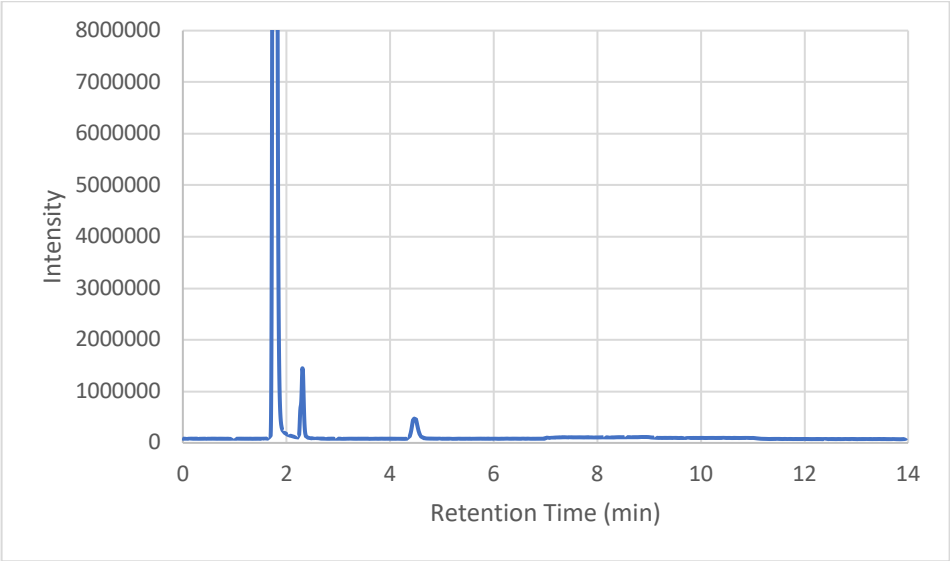

Figure S3. A representative GC spectrum of the reaction with the conditions of 48 hours, 300mg Ni/Al_2O_3, 225° C, 10 mL H_2O, 50 bar H_2, 10 mmol K_2CO_3. 1.8 min: H_2, 2.2 min N_2/air, 4.5 min CH_4.

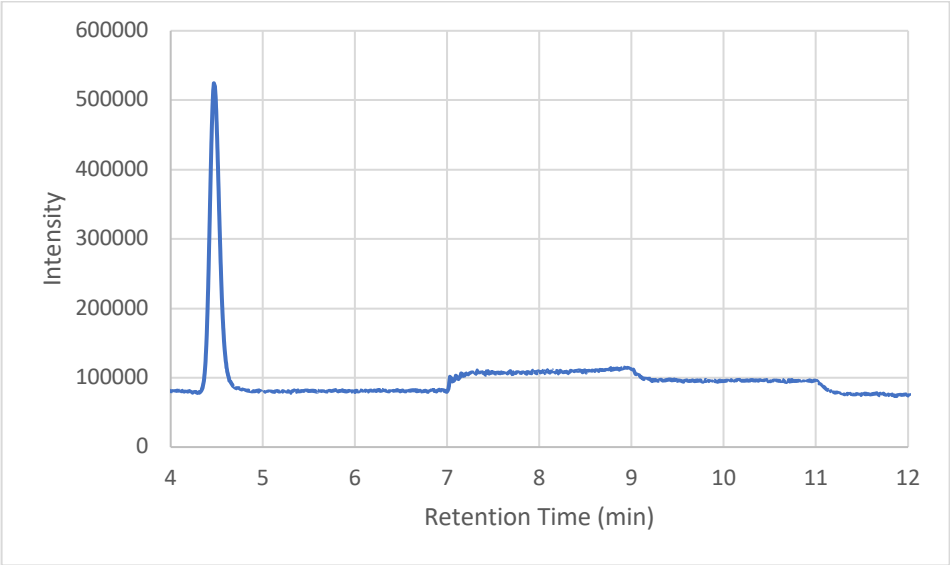

Figure S4. A representative GC spectrum of the reaction with conditions of 48 hours, 300mg Ni/Al_2O_3, 225° C, 10 mL H_2O, 50 bar H_2, 10 mmol K_2CO_3 zoomed between 4 and 12 minutes. Peak at 4.5 min corresponds to the reaction product, CH_4.

To calculate the amount of methane that was produced, the integration values were obtained from the gas chromatography spectrum. For example, the chromatograms shown in figures S3 and S4 have 99.85% H_2 and 1.15% CH_4. Nitrogen is excluded from the calculation (it is due to air present during the injection using a gas syringe). These integration values are normalized to account for their response factors. Once the response factors are accounted for the integration values are 95.75% H_2 and 4.25% CH_4. The pressure prior to releasing the gas was recorded and utilized for the next step of the calculation. The pressure of 655 psi at the time of release is multiplied by the percentage of methane. This results in 27.83 psi of methane. This is converted to atm for further computations by dividing the pressure in psi by 14.696 to obtain pressure in atm. This pressure is then used in gas law's equation to compute the amount of moles of methane as shown in equation S1. The temperature that is used for the calculation is the temperature at the time of the release of the gas. After using gas law's equation, there was 10 mmol of methane in the gas released from the reactor. This provides the 100% yield that was observed.

$$mol\ of\ methane = \frac{(1.894\ atm)(0.130\ L)}{(27.0\ ℃ + 273.15)(0.0821\ \frac{atm * L}{mol * K})}$$

Equation S1. Example calculation showing the amount of methane (mol) produced, where the volume is the volume of the reactor was (0.130 L), the temperature is the temperature at which the gas is released, and R is the ideal gas constant.

2.3 SEM/XRF data of the catalysts

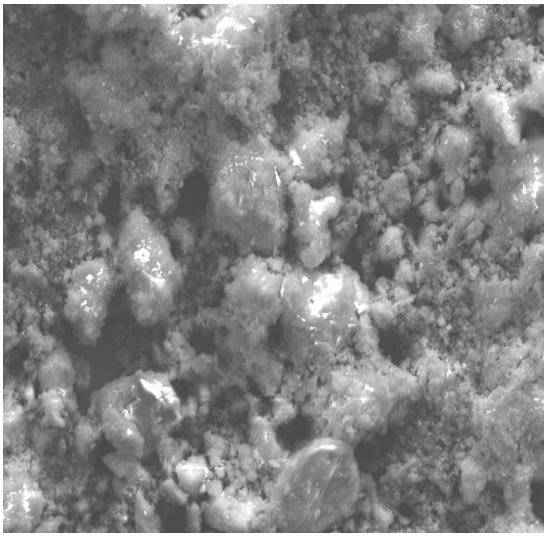

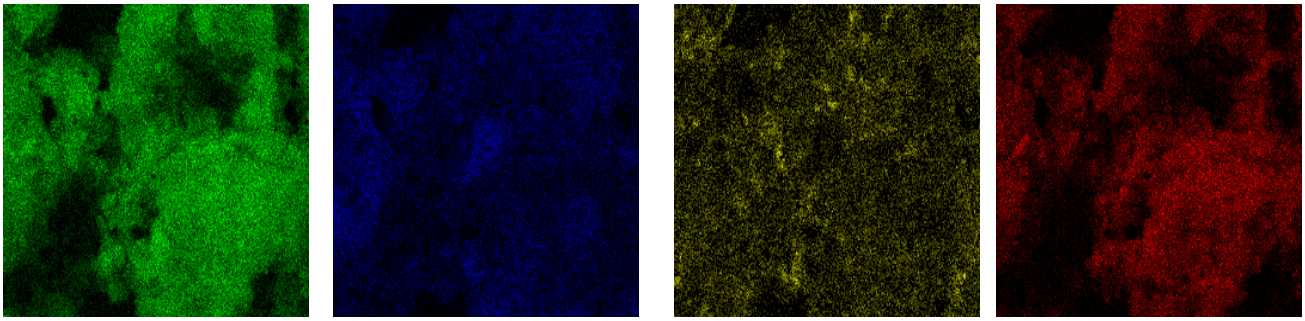

Figure S5. A SEM image and EDS mapping of the Ni/$CaAl_2O_4$ catalyst after activation

The weight concentrations were 27.4% Ni, 11.95% Ca, 38.17% Al, and 23.47% O as determined by Energy Dispersion X-Ray Spectroscopy.

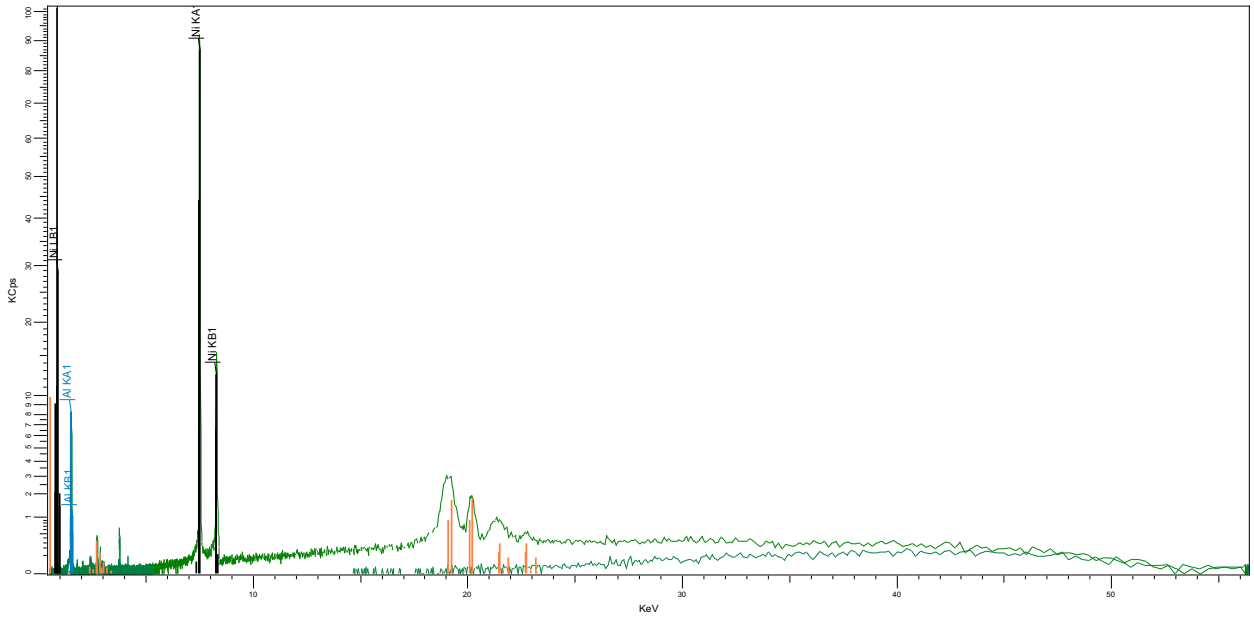

Figure S6. XRF of 25%Ni/Al_2O_3 after activation under H_2

The nickel signals are marked with black markings. Aluminum is marked with blue markings. The residual rhodium peaks are marked with orange markings. The rhodium peaks are present because the X-Ray source is rhodium.

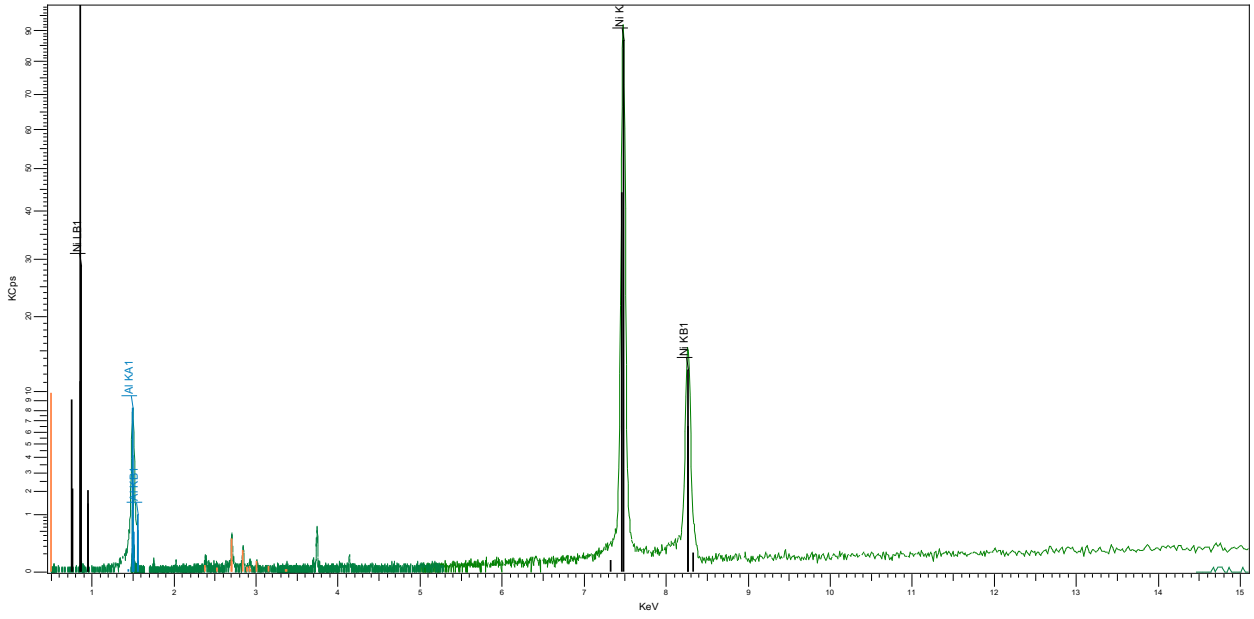

Figure S7. XRF spectra of 25%Ni/Al_2O_3 after activation zoomed into 0-15KeV

Table S2. Weight concentration of Ni/Al_2O_3

Catalyst	Nickel (%w)
Ni/Al_2O_3	25.80±0.35

2.4 NMR data

A ^{13}C NMR spectra of the solution after capture of CO_2 from the air (DAC) with KOH following the procedure described in 1.5 was collected and is presented in Figure S8. For this, a small aliquot of the solution (100 µl) was dissolved in 1 mL of D_2O. 100 mg of imidazole was used as an internal standard. The obtained peak at 164.8 ppm corresponds to a mixture of potassium bicarbonate/carbonate that was produced as a result of the capture. Nuclear Overhauser Effects were excluded from the program and the peaks were integrated to determine the amount of CO_2 captured.

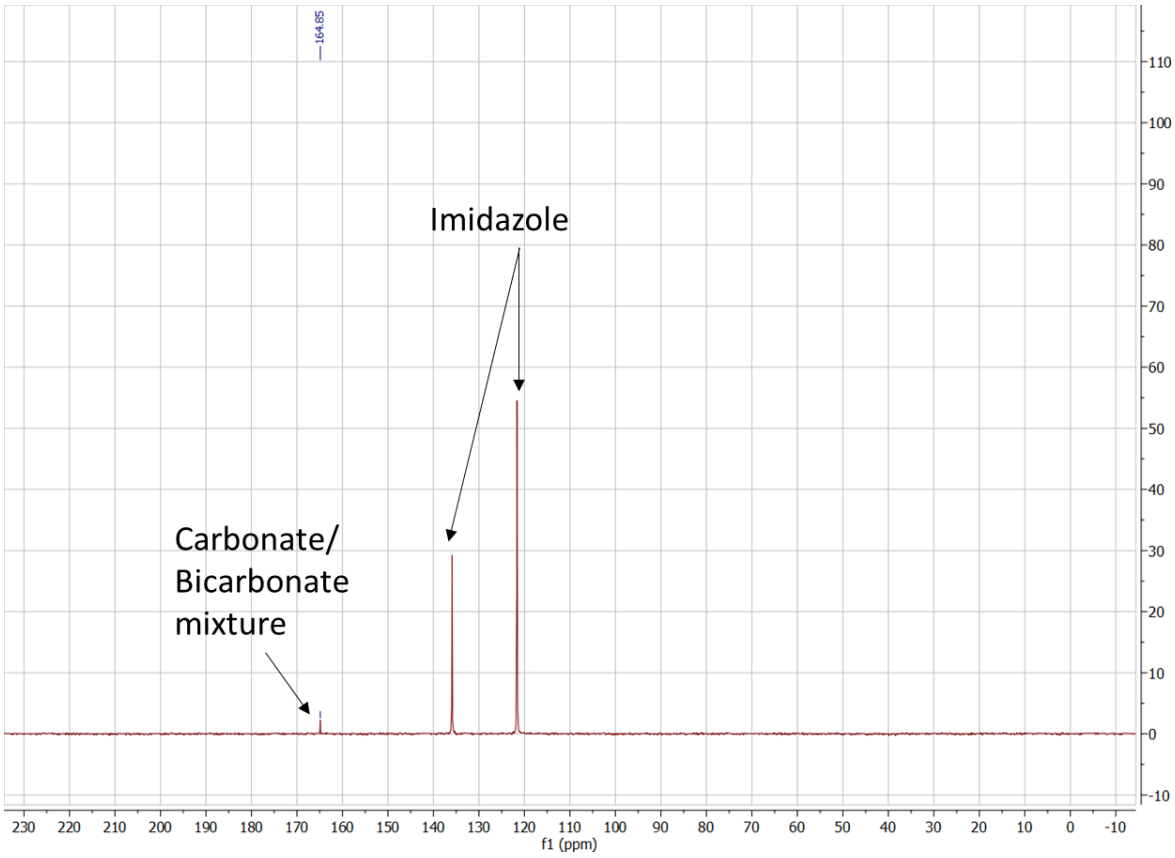

Figure S8. Proton decoupled ^{13}C NMR of the DAC solution after capture (in D_2O with imidazole as internal reference).

Figure S9 shows the proton decoupled ^{13}C NMR spectra of a 1/1 mixture of potassium carbonate/potassium bicarbonate ($K_2CO_3/KHCO_3$), whose ^{13}C signals appear as a single peak in D_2O at 164.04 ppm. Imidazole was used as the internal standard. This peak matches closely the peak shown in Figure S8.

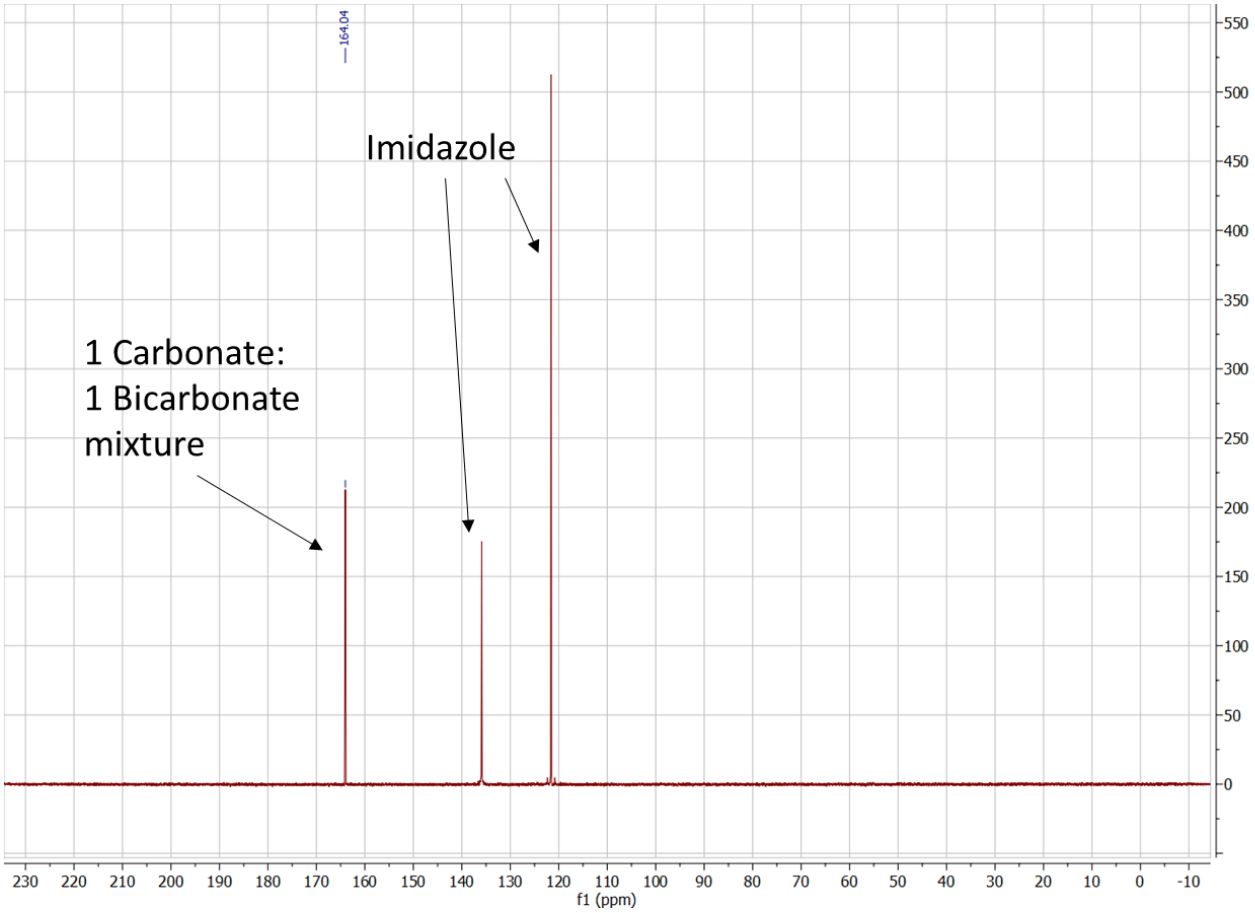

Figure S9. Proton decoupled ^{13}C NMR of a 1:1 mixture of potassium carbonate/potassium bicarbonate (in D_2O with imidazole as internal reference).

Figure S10 shows the ^{13}C NMR spectra of a sample of potassium bicarbonate, $KHCO_3$, in D_2O. Imidazole was used as the internal standard.

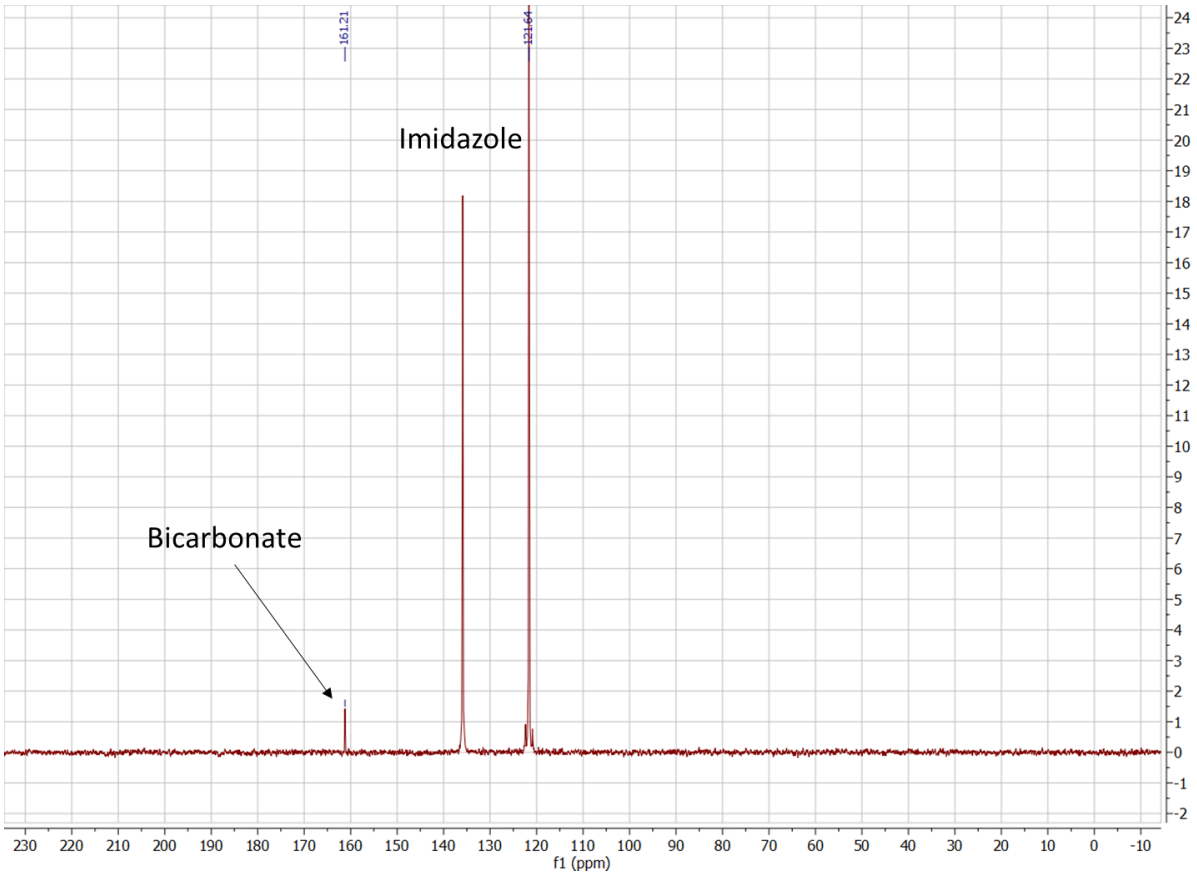

Figure S10. Proton decoupled ^{13}C NMR of a potassium bicarbonate, $KHCO_3$ (in D_2O with imidazole as internal reference)

Figure S11 shows the Proton decoupled ^{13}C NMR spectra of a sample of potassium carbonate, $K_2{}^{13}CO_3$, in D_2O. Imidazole was used as the internal standard.

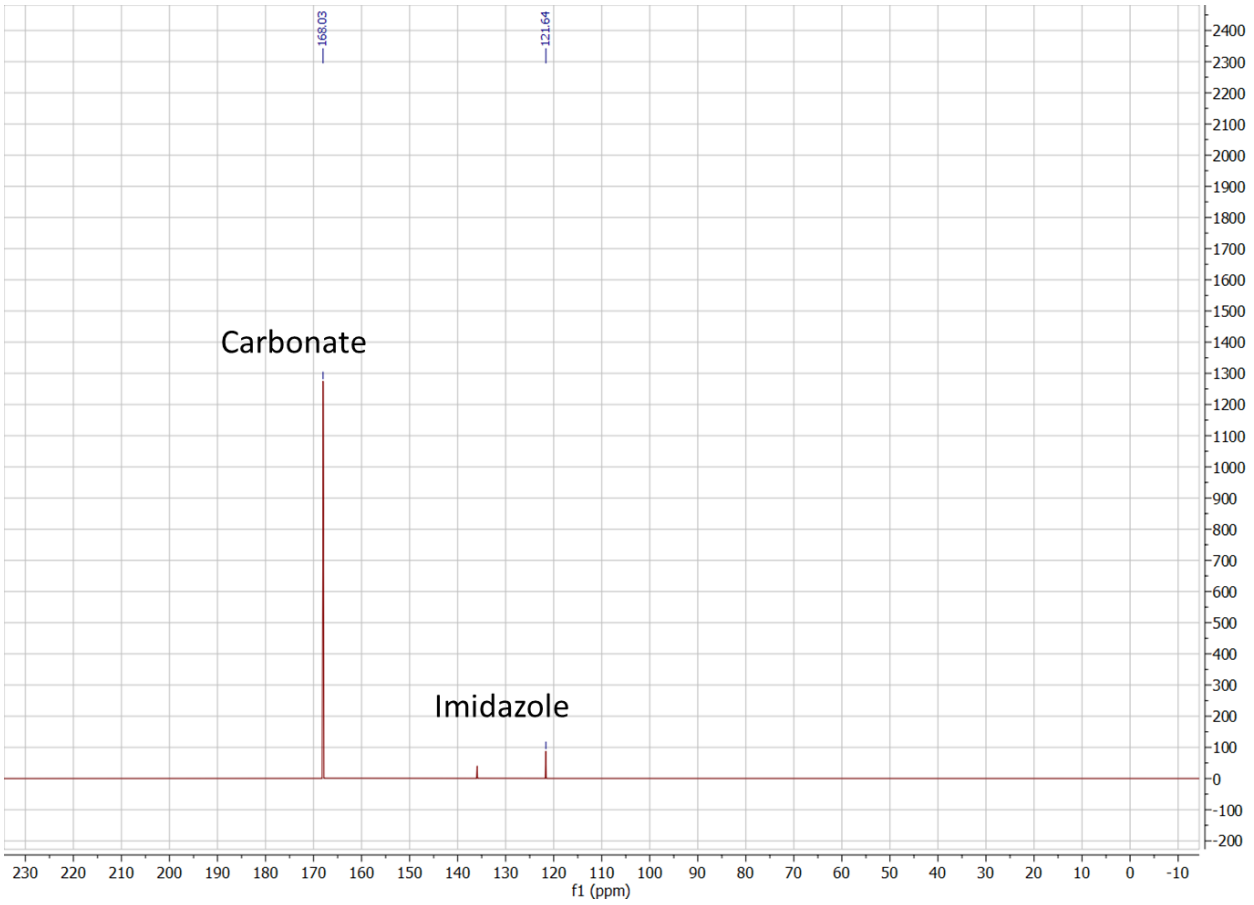

Figure S11. Proton decoupled ^{13}C NMR of potassium carbonate, $K_2{}^{13}CO_3$ (in D_2O with imidazole as internal reference)

A reaction with ^{13}C labeled $K_2{}^{13}CO_3$ was performed to determine whether the resulting methane would be ^{13}C-labelled (following the condition in Table 3, entry 3). For this, part of the gas mixture after the reaction with $K_2{}^{13}CO_3$ was bubbled through a solution of deuterated toluene and a ^1H NMR spectrum was collected. Methane is known to appear at about 0.17 ppm in toluene-d_8. [1,2] With ^{13}C-labelled methane, the methane peak would appear as a doublet. And this was indeed what was observed in the spectrum (Figure S12 and S13 A), showing that the methane resulting from the reaction was ^{13}C-labelled. The $^1J_{CH}$ value obtained was equal to 125.7 Hz. There was also a trace amount of ^{12}C-methane (due to the presence of $K_2{}^{12}CO_3$ in the carbonate which was 98.7% ^{13}C according to the manufacturer).

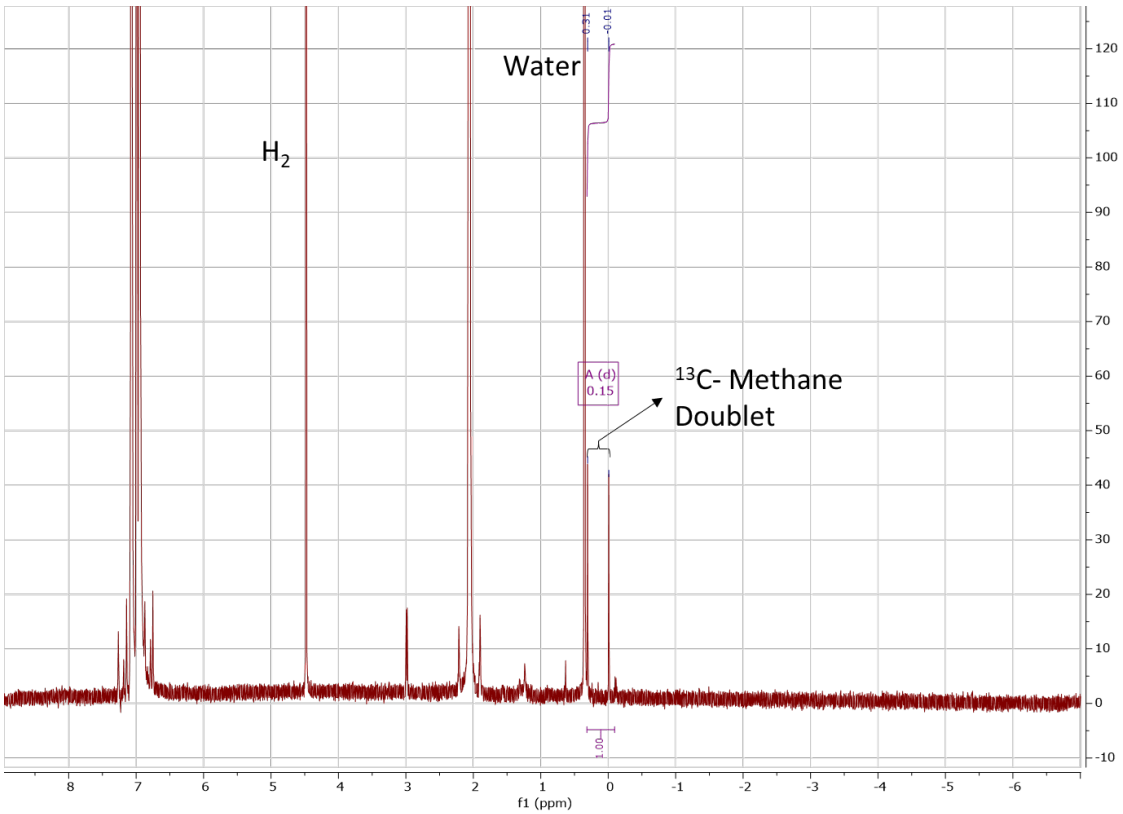

Figure S12. ^{1}H NMR of the gas mixture after reaction with $K_2{}^{13}CO_3$ showing the ^{13}C-methane peaks around 0.17 ppm (as well as the peak corresponding to H_2 at 4.48 ppm due to the presence of H_2 in the gas phase) in toluene-d_8. The expansion of the methane region is shown in Figure S13 A.

Following a similar procedure, where methane from the reaction mixture is bubbled through deuterated toluene to obtain a methane signal, ^{1}H NMR was also obtained for pure ^{13}C-methane and ^{12}C-methane to confirm that the methane in the reaction gas mixture was ^{13}C labelled. Figure S13-C shows that the ^{12}C-methane peak is at 0.16 ppm. Figure S13-A and S13-B show the $^{13}CH_4$ peaks in the same positions (~0.01 and 0.31 ppm) and with the same $^{1}J_{CH}$ coupling constant of 125.7 Hz. Thus, it was confirmed that we can synthesize ^{13}C labelled methane from ^{13}C labelled carbonate salts.

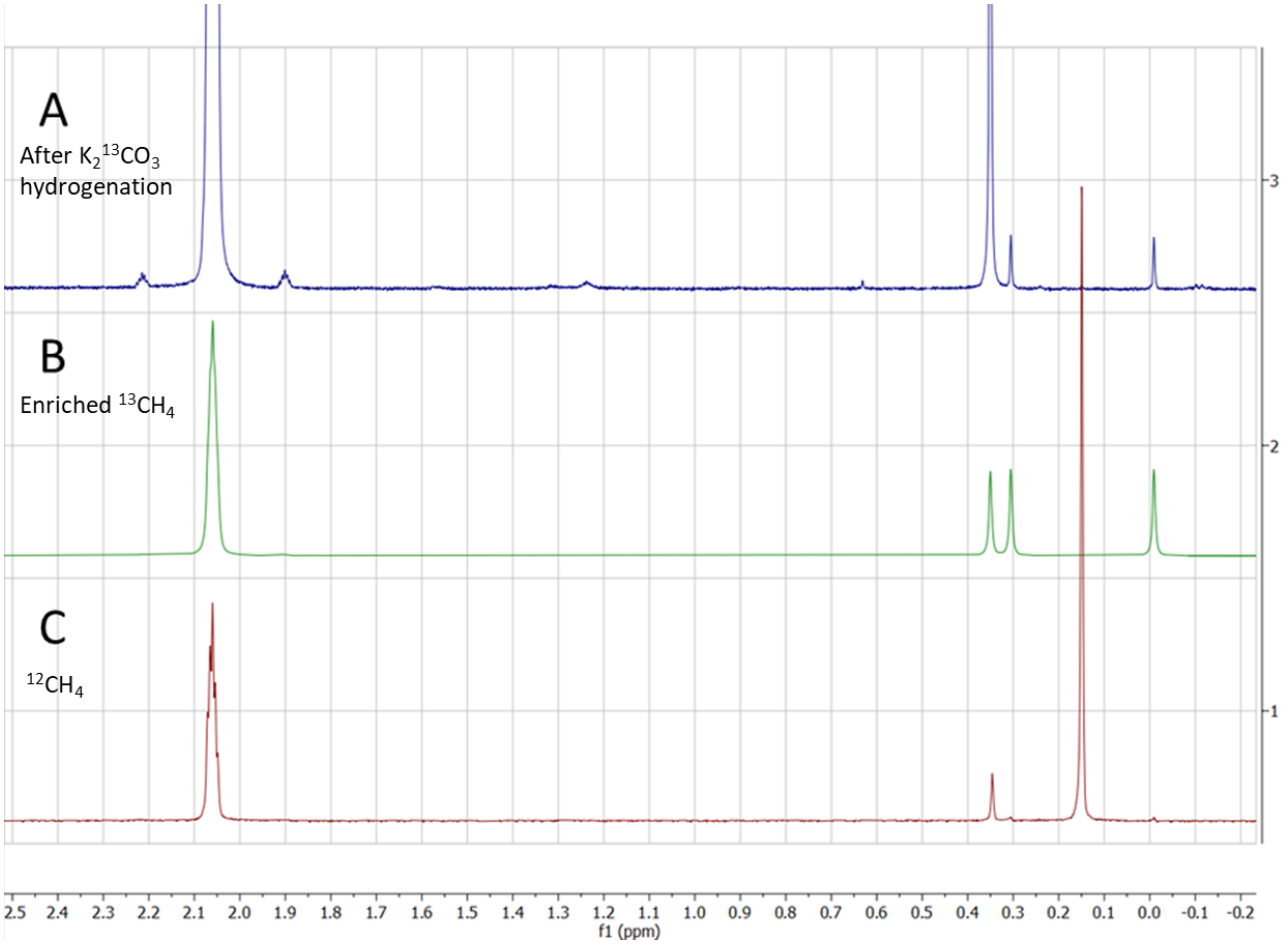

Figure S13. ^{1}H NMR of methane in toluene from various methane sources shown from -0.2 ppm to 2.5 ppm [A] from reaction gas mixture as shown in Figure S12 [B] from 99% ^{13}C pure ^{13}C-methane [C] From ^{12}C-methane. Taken in toluene-d_8.

A ^{13}C NMR spectrum was also collected after the reaction with $K_2{}^{13}CO_3$ to determine whether the resulting methane was ^{13}C-labelled (Figure S14). The gas mixture after the reaction was bubbled through a solution of deuterated toluene. There is a peak at 0 ppm, which corresponds to methane, as verified by analyzing 99% ^{13}C methane (Figure S15).

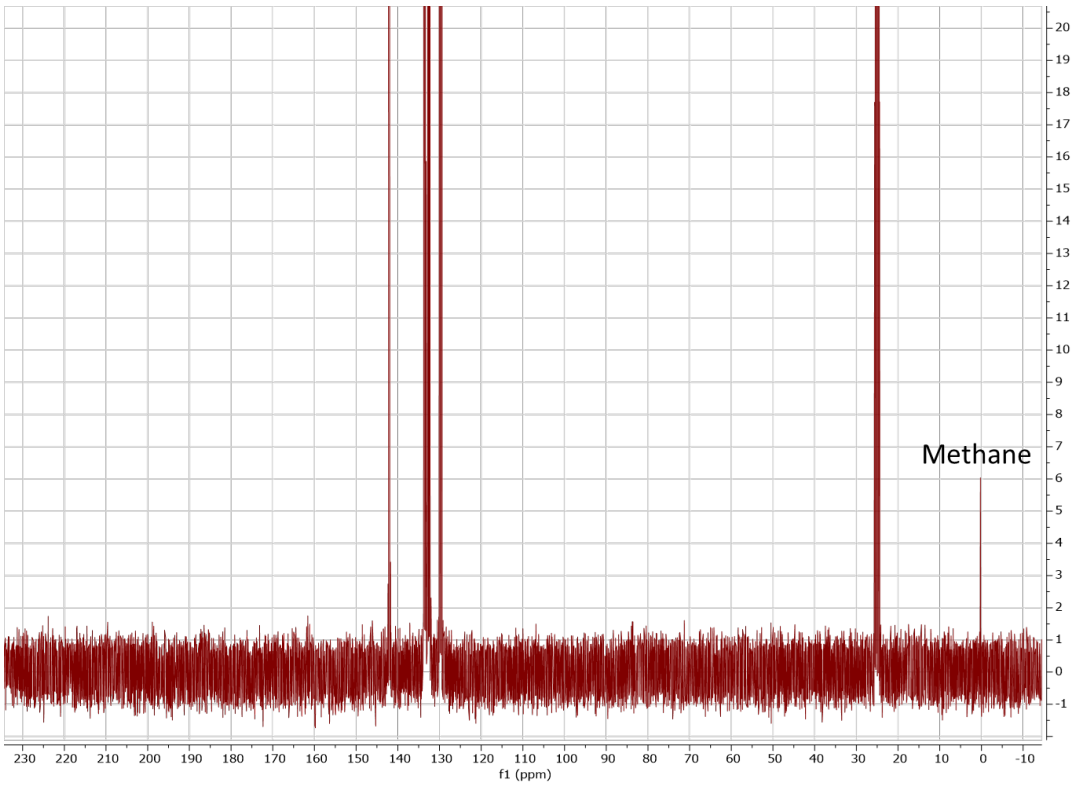

Figure S14. Proton decoupled ^{13}C NMR of the gas mixture after reaction with $K_2{}^{13}CO_3$ showing the ^{13}C-methane peaks around 0 ppm. Taken in toluene-d_8.

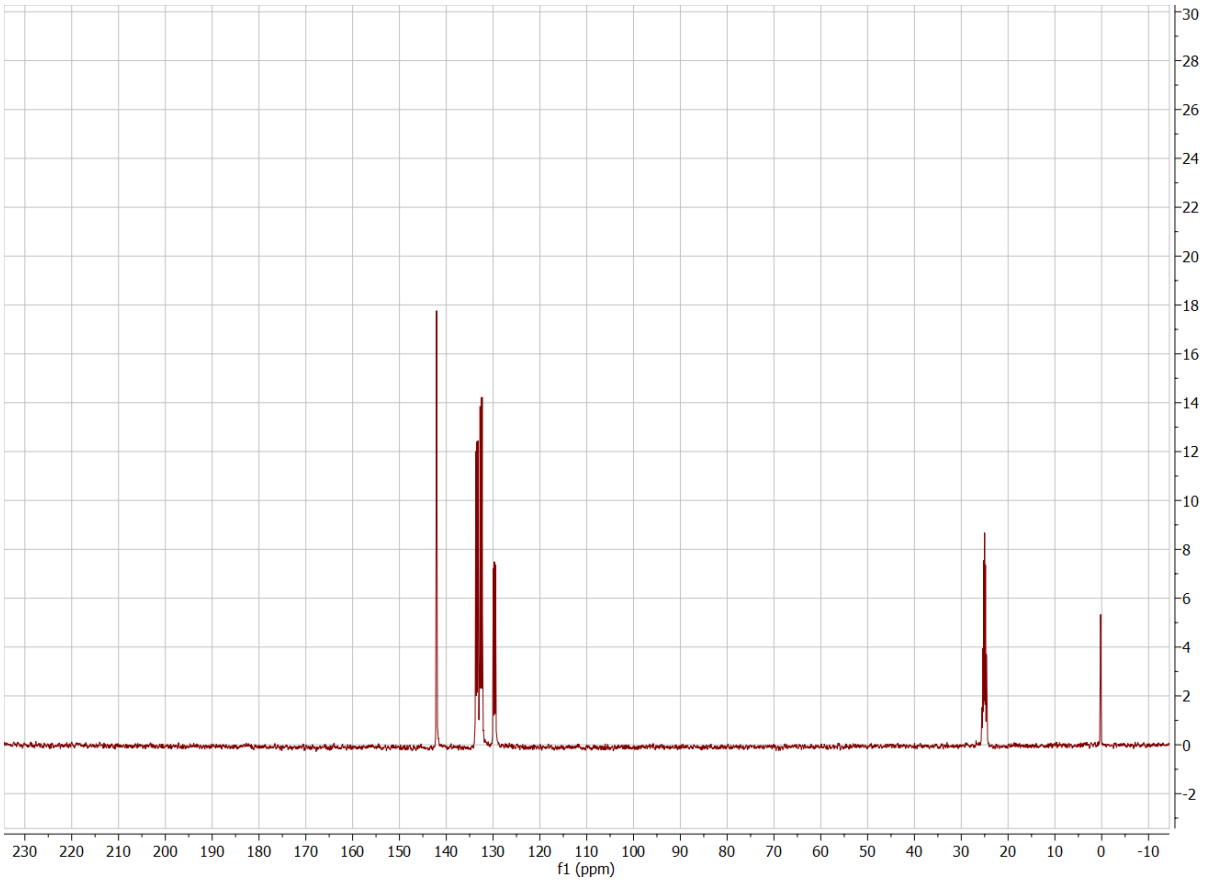

Figure S15. Proton decoupled ^{13}C NMR of $^{13}CH_4$ (99% ^{13}C) showing the ^{13}C-methane peaks around 0 ppm. Taken in toluene-d_8.

References

(1) Chen, J. Y. C.; Martí, A. A.; Turro, N. J.; Komatsu, K.; Murata, Y.; Lawler, R. G. Comparative NMR Properties of H_2 and HD in Toluene-d_8 and in H_2/HD@C60. *Journal of Physical Chemistry B* **2010**, *114* (45), 14689–14695. https://doi.org/10.1021/jp102860m.

(2) Fulmer, G. R.; Miller, A. J. M.; Sherden, N. H.; Gottlieb, H. E.; Nudelman, A.; Stoltz, B. M.; Bercaw, J. E.; Goldberg, K. I. NMR Chemical Shifts of Trace Impurities: Common Laboratory Solvents, Organics, and Gases in Deuterated Solvents Relevant to the Organometallic Chemist. *Organometallics* **2010**, *29* (9), 2176–2179. https://doi.org/10.1021/om100106e.